LETTERS
https://doi.org/10.1038/s41477-018-0318-3
nature plants

Mechanistic framework for cell-intrinsic re-establishment of PIN2 polarity after cell division

Matouš Glanc[1,2], Matyáš Fendrych[1,2] and Jiří Friml[1*]

Cell polarity, manifested by the localization of proteins to distinct polar plasma membrane domains, is a key prerequisite of multicellular life. In plants, PIN auxin transporters are prominent polarity markers crucial for a plethora of developmental processes. Cell polarity mechanisms in plants are distinct from other eukaryotes and still largely elusive. In particular, how the cell polarities are propagated and maintained following cell division remains unknown. Plant cytokinesis is orchestrated by the cell plate—a transient centrifugally growing endomembrane compartment ultimately forming the cross wall[1]. Trafficking of polar membrane proteins is typically redirected to the cell plate, and these will consequently have opposite polarity in at least one of the daughter cells[2–5]. Here, we provide mechanistic insights into post-cytokinetic re-establishment of cell polarity as manifested by the apical, polar localization of PIN2. We show that the apical domain is defined in a cell-intrinsic manner and that re-establishment of PIN2 localization to this domain requires de novo protein secretion and endocytosis, but not basal-to-apical transcytosis. Furthermore, we identify a PINOID-related kinase WAG1, which phosphorylates PIN2 in vitro[6] and is transcriptionally upregulated specifically in dividing cells, as a crucial regulator of post-cytokinetic PIN2 polarity re-establishment.

Cells in the *Arabidopsis* root meristem are a perfect model to study cell polarity as they possess at least four distinct plasma membrane domains marked by the asymmetric accumulation of different cargoes[7] (Fig. 1a). Among these, PIN2 in the epidermis is particularly interesting for its pronounced apical polarity, which is crucial for shootward auxin transport and root gravitropism[8,9]. It has been reported that during cytokinesis, plasma membrane cargoes, including polarly localized ones, localize to the cell plate[2–5,10]. To dissect which trafficking pathways were responsible for cell plate cargo delivery we utilized the Dendra photoconvertible marker[11]. When we photoconverted functional (Supplementary Fig. 1) PIN2-Dendra or Dendra-PIP1;4 from green to red before cytokinesis, we observed the contribution of both de novo secretion and endocytic recycling to the cell plate, (Fig. 1b,c, Supplementary Fig. 1 and Supplementary Video 1), consistently with previous findings[10]. It was reported that in newly divided cells, PIN2 is localized at both sides of the cross wall[4]. Thus, the rerouting of endomembrane trafficking during cytokinesis results in apolar localization of the otherwise strictly polar PIN2[4,12].

When is apical PIN2 localization subsequently re-established, and which cellular mechanisms are required for this process? There was no difference in *PIN2* promoter activity between the daughter cells (Supplementary Fig. 1), implying post-transcriptional regulation. To address the dynamic changes of subcellular PIN2 localization, live-cell imaging is indispensable since time is the decisive variable. However, exact determination of PIN2 polar localization dynamics is difficult using *PIN2::PIN2-XFP* reporter lines, since the original apical domain is pre-occupied with molecules inherited from the mother cell, conventional microscopy cannot distinguish between adjacent newly formed plasma membranes due to the diffraction limit, and super-resolution techniques are limited in time lapse potentiality and throughput. To overcome these limitations, we expressed *PIN2-GFP* from the cytokinesis-specific *KNOLLE* promoter[13] and performed time lapse imaging. This approach enabled us to observe the trafficking fate of molecules synthesized in a narrow time window during and immediately after the cytokinetic event (Fig. 1d,e and Supplementary Video 2). In recently divided cells, the KN::PIN2-GFP signal could be observed almost exclusively at the cell plate or new plasma membrane, further confirming redirection of secretion to the cell plate during cytokinesis[12], but also afterwards (Fig. 1d,e). At 1–2 hours after cytokinesis, KN::PIN2-GFP signal was still strongest at the newly formed membrane pair but started to appear also at the apical and lateral domains of the upper cell. By 3–5 hours after cytokinesis, the signal clearly localized to the apical domains of both daughter cells, marking completed polarity re-establishment (Fig. 1e,f). *KN::PIN2-GFP* only non-significantly rescued root gravitropism in the *pin2* mutant, did not affect the phenotype of *Col-0*, and its signal intensities at newly formed plasma membranes were comparable with those in a complementing *PIN2::PIN2-GFP* line (Supplementary Fig. 1), suggesting that the observed localization was not an overexpression artefact.

Taken together, these results confirm that during and immediately after cytokinesis, virtually all membrane traffic of both daughter cells is redirected to the cell plate[12], creating a situation in which the lower cell has a correctly, that is apically localized, PIN2, but the upper daughter cell has an ectopic basally localized pool of PIN2, in addition to the apical pool inherited from the mother cell[4]. Therefore, the cell must possess a mechanism to re-establish proper localization of PIN2 and other polar proteins (Fig. 1a).

In plants, cell fate is determined by positional information conveyed by numerous intercellular signalling molecules[14]. We therefore tested whether tissue context and cell-to-cell signalling is required for re-establishment of cell polarity after cytokinesis. In other developmental contexts, for example during organogenesis or vascularization, auxin itself serves as a polarizing cue for the localization of PIN proteins[15,16]; therefore, we first tested whether post-cytokinetic polarity re-establishment is regulated by auxin levels in cells or its directional flow across the tissue. Nonetheless, PIN2 polarity developed normally in *KN::PIN2-GFP* roots when we exogenously applied the natural auxin indole-3-acetic acid (IAA) (Supplementary Figs. 2 and 6). In plants treated with the auxin transport inhibitor naphthylphthalamic acid (NPA)[17],

[1]IST Austria, Klosterneuburg, Austria. [2]Department of Experimental Plant Biology, Faculty of Science, Charles University, Prague, Czech Republic.
*e-mail: jiri.friml@ist.ac.at

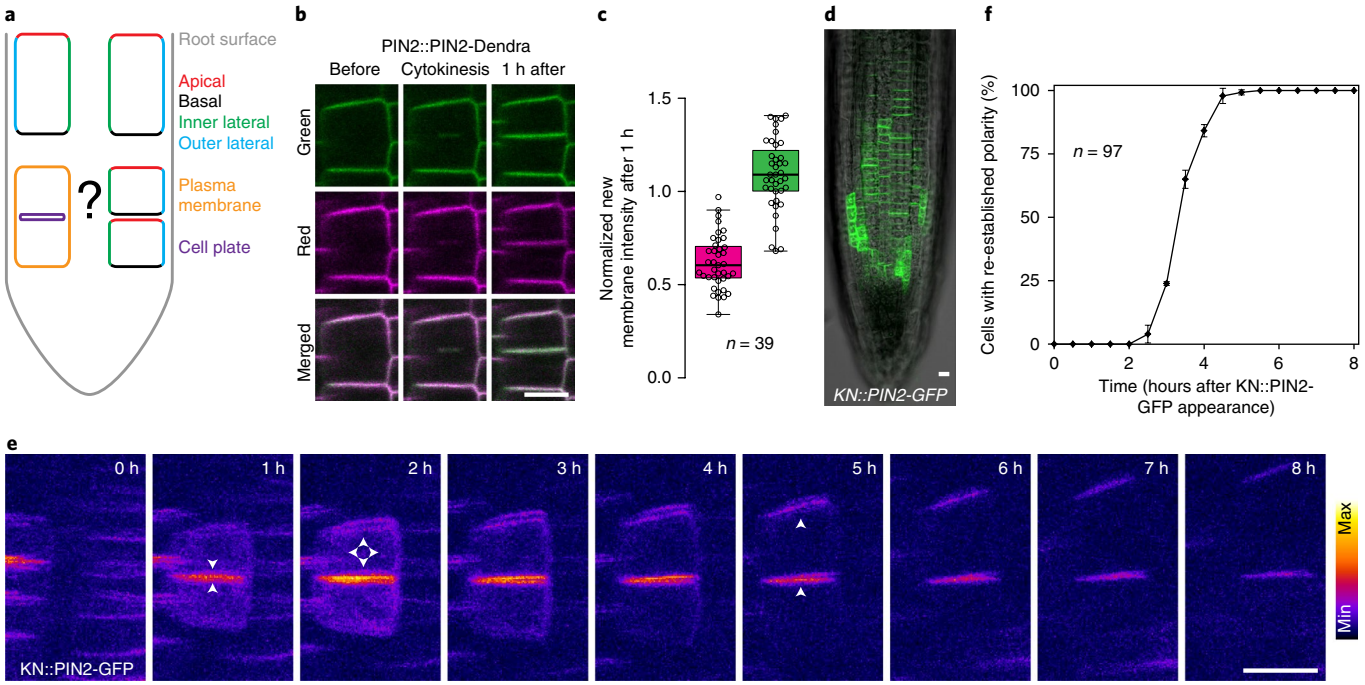

Fig. 1 | Cell polarity needs to be re-established after cytokinesis. a, Cells in the *Arabidopsis* root possess at least four distinct plasma membrane domains: apical, basal, inner lateral and outer lateral[7]. During cytokinesis, virtually all membrane traffic is redirected to the cell plate[12], implying that the daughter cells must have a mechanism to re-establish polarity afterwards. **b**, Both pre-existing (magenta) and newly synthesized (green) pools of PIN2-Dendra localize to the cell plate and newly formed plasma membrane in cells that were photoconverted before the onset of cytokinesis. **c**, Quantification of **b**. The graph shows signal intensity at the newly formed plasma membrane 1 h after cytokinesis normalized to the intensity of the neighbouring, old plasma membranes in both red and green channels; higher relative intensity of the green channel confirms predominant contribution of de novo secretion to the cell plate protein pool. The box plot represents median, 1st and 3rd quartile; the whiskers extend to data points <1.5 interquartile range away from the 1st or 3rd quartile; all data points are shown as circles. *n* indicates the number of cells from eight roots and three independent experiments. **d**, Expression pattern of the *KN::PIN2-GFP* construct in the root meristem. The experiment was repeated independently more than three times with similar results. **e**, A time series of a single newly divided cell pair expressing *KN::PIN2-GFP*. Up to 1 h after cytokinesis, signal is almost exclusively at the cell plate. At 1–3 h after cytokinesis, signal appears at all plasma membrane domains, and typical apical polar distribution pattern is re-established 2–5 h after cytokinesis. Arrowheads indicate predominant signal localization. **f**, Quantitative analysis of the dynamics of KN::PIN2-GFP polarity re-establishment. The timepoint at which both daughter cells had clearly apically localized KN::PIN2-GFP signal (between 4 and 5 h in the case of the cell pair shown in **e**) was scored for each cell pair, and the percentage of cell pairs with re-established polarity was plotted against time. The graph shows mean ± s.d. of three independent experiments, *n* indicates the total number of cell pairs. The number of roots/cell pairs analysed in each experiment was 5/47, 3/30 and 2/20, respectively. Scale bars, 10 µm.

apical polarity was established correctly, but with a significant delay (Fig. 2a,b,e and Supplementary Fig. 6).

To test more generally for a requirement of tissue context, we separated the *KN::PIN2-GFP* root meristematic and transition zone from, (1) the root tip, (2) the differentiation zone and the rest of the plant or (3) both. The pattern of cell division occurrence and orientation was disturbed as described before[18] but PIN2 polarity re-establishment remained unaffected (Supplementary Figs. 2 and 6), suggesting that this process does not depend on long-range cell-to-cell signalling. To address the importance of short-range signalling, we isolated small patches of cells from their neighbours by laser ablation. We could still observe normal re-establishment of apical PIN2 polarity in isolated patches of as few as three cells (Fig. 2c–e and Supplementary Fig. 6), arguing against the influence of short-range signalling.

Together, these results indicate that while auxin transport and/or signalling can affect PIN trafficking and polarity, presumably through transcriptional reprogramming[16], neither polarized auxin flow nor other cell-to-cell signalling pathways are primary cues defining apical–basal polarity in newly divided root cells. Therefore, post-cytokinetic polarity re-establishment must be governed by an unknown cell-intrinsic mechanism instead.

We next addressed the cellular machinery that executes PIN2 polarity re-establishment. To test whether the ectopic basal PIN2 molecules were delivered to the apical domain by transcytosis (trafficking-based protein translocation between polar domains)[19], we created a *KN::PIN2-Dendra* line, photoconverted newly divided cell pairs and followed them during polarity re-establishment. The apical signal distribution pattern developed in both channels showing contribution of both pre-existing PIN2 molecules (in magenta) and the de novo synthesized PIN2 (in green) (Fig. 3a,b). However, after photoconversion, when we photobleached the red signal from the endosomes and all cell sides except the new, cell plate-derived plasma membranes, we did not observe a considerable apical signal in the red channel (Fig. 3c,d), which argues against a substantial contribution of basal-to-apical PIN2 transcytosis to polarity establishment in this context. Furthermore, only weak, presumably lateral diffusion-based, redistribution of red signal was observed after photoconversion of the new plasma membrane domain in *PIN2::PIN2-Dendra*, and the apical signal was not restored in *KN::PIN2-GFP* cells treated with the translation inhibitor cycloheximide (Supplementary Figs. 3 and 6). Finally, treatment with the ARF GEF inhibitor brefeldin A prevented PIN2 polarity re-establishment of *KN::PIN2-GFP* in the *big3* mutant, where it inhibits secretion[12], but not in the wild type

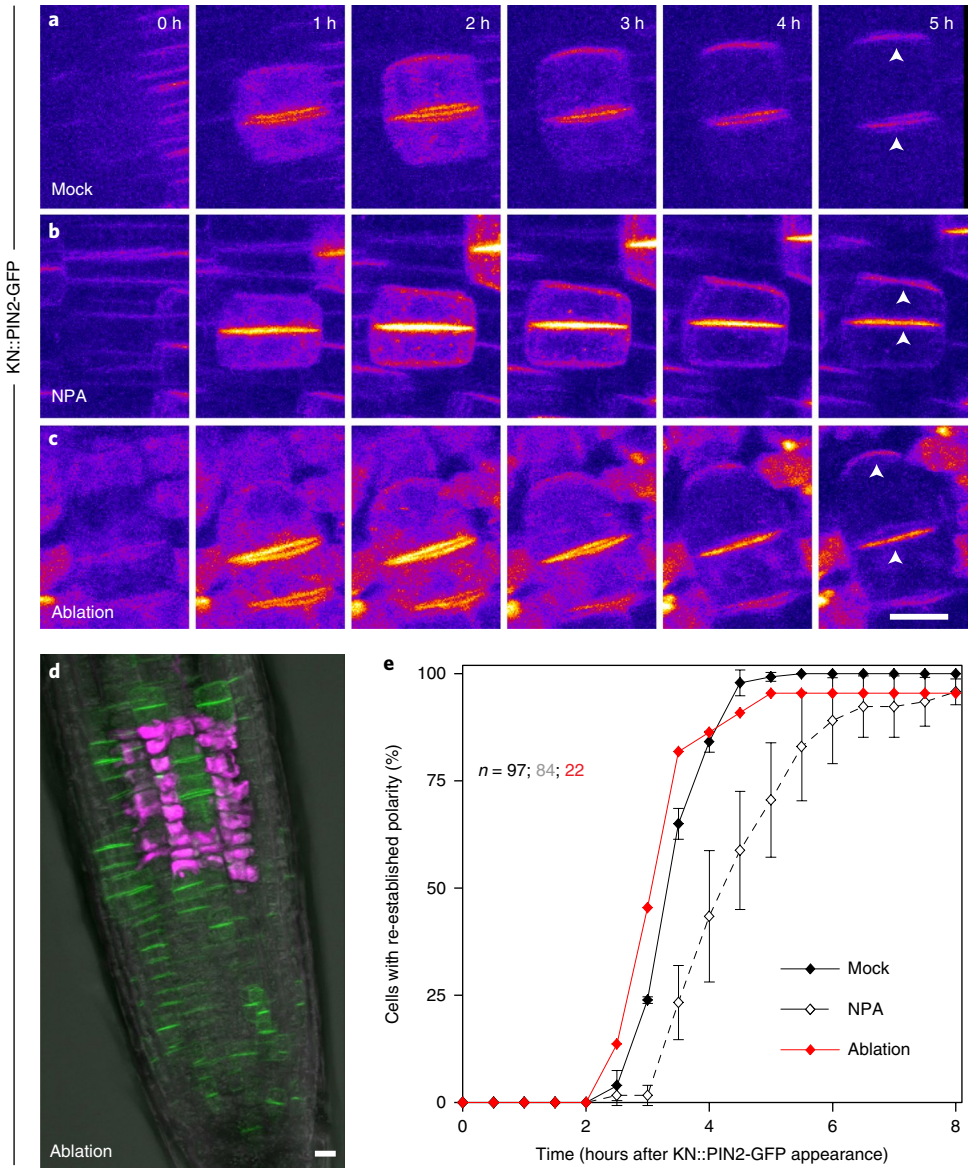

Fig. 2 | Apical–basal polarity of newly divided cells is established in a cell-intrinsic manner. a,**b**, Re-establishment of apical PIN2 polarity in *KN::PIN2-GFP* plants treated with the auxin transport inhibitor NPA, **b** is qualitatively not altered compared with the mock control **a**. **c**, Laser ablation of surrounding cells does not prevent the re-establishment of apical PIN2 polarity. **d**, *KN::PIN2-GFP* expressing root in which laser-ablated cells are marked by the uptake of propidium iodide (magenta). The experiment was repeated independently three times with similar results. **e**, Quantitative analysis of the dynamics of KN::PIN2-GFP polarity re-establishment in **a**–**c**. NPA treatment causes a delay of polarity re-establishment compared with the control, while laser ablation of surrounding cells has no effect. The control is the same as in Fig. 1f. The graph shows mean ± s.d. of three independent experiments, *n* indicates the total number of cell pairs. The number of roots/cell pairs analysed in each experiment was 4/20, 4/35 and 3/29 in **b** and 3/9, 1/5 and 4/8 in **c**, respectively. Due to the smaller sample size of **c** caused by technical limitations, values from all experiments were pooled and analysed together. Arrowheads indicate apical polar localization of PIN2-GFP. Scale bars, 10 µm.

(Supplementary Figs. 3 and 6). Taken together, these data demonstrate that re-establishment of PIN2 apical polarity depends on secretion of de novo synthesized PIN2 molecules but not on their basal-to-apical transcytosis.

Ectopic basal and lateral PIN2 molecules need to be removed from the plasma membrane during polarity re-establishment. Polarity of PINs has been linked to their slower lateral diffusion within the plasma membrane[4,20–22]. We therefore speculated that higher PIN2 mobility in the new plasma membrane domain might contribute to PIN2 removal and polarity re-establishment and tested this with fluorescence recovery after photobleaching experiments. We did observe slightly higher PIN2 fluorescence recovery after photobleaching rates in the newly formed membranes compared with the old ones; however, the differences were significant only in *PIN2::PIN2-GFP*, but not in *PIN2::PIN2-mCherry* (Supplementary Fig. 4). We therefore conclude that the observed differences reflected differential properties of the fluorophores rather than of the cargo, and that specific lateral diffusion properties probably do not play a major role in PIN2 polarity re-establishment.

A link between clathrin-mediated endocytosis (CME) and PIN polarity[23], as well as post-cytokinetic PIN2 polarity re-establishment, has previously been proposed[3,4]. However, strong pleiotropic defects of the mutants used in these studies make it difficult to dissect direct and indirect effects. To re-examine the role of CME in

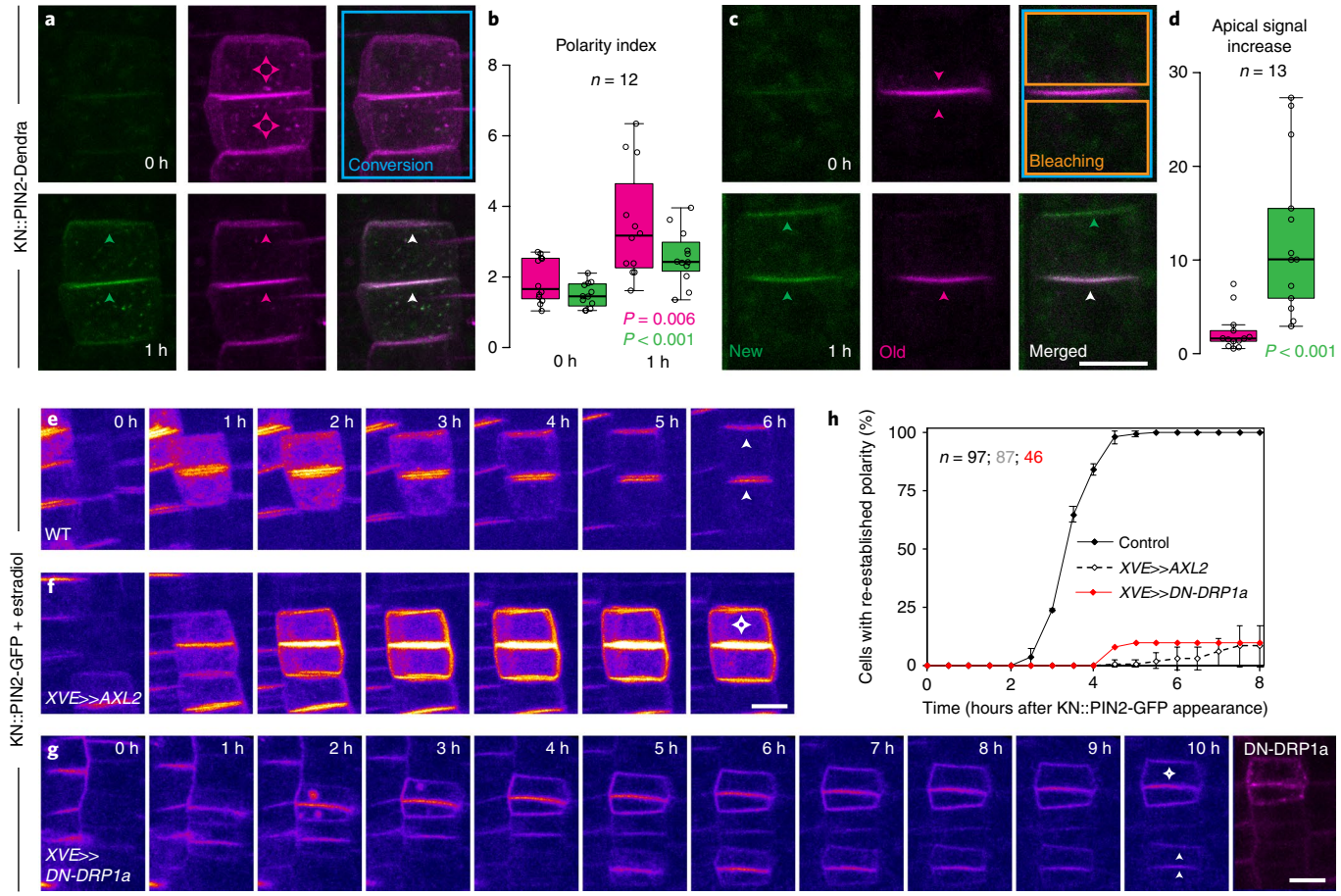

Fig. 3 | PIN2 apical polarity re-establishment requires secretion and endocytosis, but not transcytosis. a, A newly divided cell pair of *KN::PIN2-Dendra* that was photoconverted before polarity re-establishment. Within 1 h following photoconversion, apical polar distribution of both newly synthesized (green) and pre-existing (magenta) PIN2-Dendra pools can be observed. **b**, Quantitative analysis of **a**. The value of the polarity index (ratio of signal intensity at the apical plasma membrane/lateral plasma membrane of the upper cell) significantly increased in both channels within 1 h following photoconversion. $n = 12$ cell pairs from 11 roots in four independent experiments. **c**, A similar experiment as in **a** with an additional step where all signal, except that at the new membrane pair, was photobleached immediately after photoconversion. In this case, apical polarity develops only in the green channel. **d**, Quantification of **c**. The graph shows the increase in red and green signal intensity at the apical plasma membrane of the upper cell within 1 h following photoconversion and photobleaching. The larger signal increase in the green channel indicates predominant contribution of de novo secretion to polarity re-establishment. $n = 13$ cells from nine roots in three independent experiments. Arrowheads indicate predominant localization of PIN2-Dendra in the corresponding channel; white, both channels. **e**,**f**, Inhibition of endocytosis by estradiol-inducible overexpression of Auxilin-like2 in *KN::PIN2-GFP* cells caused prolonged residence of signal at the plasma membrane and abolished the cells' ability to re-establish apical PIN2 polarity. **g**, Apical polarity re-establishment in *KN::PIN2* × *XVE»DN-DRP1a-mRFP* after estradiol treatment. Thanks to patchy expression of the construct (see the last frame), cells with high levels of DN-DRP1a-mRFP that fail to re-establish apical polarity could be seen alongside cells with low levels, where polarity re-establishment proceeded normally. **h**, Quantitative analysis of **e**–**g**. The control is the same as in Fig. 1f. The graph shows mean ± s.d. of three (**f**), mean of two (**g**) independent experiments, *n* indicates the total number of cell pairs. The number of roots/cell pairs analysed in each experiment was 4/29, 6/38 and 3/20 in **f** and 3/21 and 4/25 in **g**, respectively. Arrowheads indicate predominant localization of PIN2-GFP. Box plots represent median, 1st and 3rd quartile; the whiskers extend to data points <1.5 interquartile range away from the 1st or 3rd quartile; all data points are shown as circles. *P*-values were calculated using two-tailed two-sample t-test with unequal variance. Scale bars, 10 µm.

PIN2 polarity re-establishment, we conditionally inhibited endocytosis by inducible overexpression of the putative clathrin-uncoating factor Auxilin-like2[24]. In *KN::PIN2-GFP* x *XVE»AXL2* plants treated with estradiol, most cells completely lost the ability to polarize PIN2 (Fig. 3f,h, Supplementary Fig. 6 and Supplementary Video 3), while polarity re-establishment proceeded normally in estradiol-treated *KN::PIN2-GFP* (Fig. 3e) and mock-treated *KN::PIN2-GFP* x *XVE»AXL2* (data not shown) controls. Inducible overexpression of a dominant-negative version of Dynamin-related protein 1 A (DRP1a)[5] led to the same result (Fig. 3g,h and Supplementary Fig. 6), confirming the direct requirement of functional CME for post-cytokinetic PIN2 polarity re-establishment.

Multiple approaches have confirmed that (de)phosphorylation of PIN proteins by PINOID (PID) and its homologues WAG1 and WAG2 regulates their apical–basal localization[6,25–28]. PIN2 polarity re-establishment in the *KN::PIN2^{S3A}-GFP* with three PID-phosphorylated serines S237, S258 and S310 mutated to alanines[6] showed a delay in polarity re-establishment compared with the *KN::PIN2-GFP* control (Supplementary Figs. 5 and 6); however, introducing *KN::PIN2-GFP* into the *pid wag1 wag2* loss-of-function mutant[6] led to complete PIN2 polarity re-establishment failure (Fig. 4a–c, Supplementary Fig. 6 and Supplementary Video 4). Therefore, PID and WAG kinases mediate PIN2 polarity re-establishment by phosphorylating S237, S258 and S310, but also other PIN2 residues

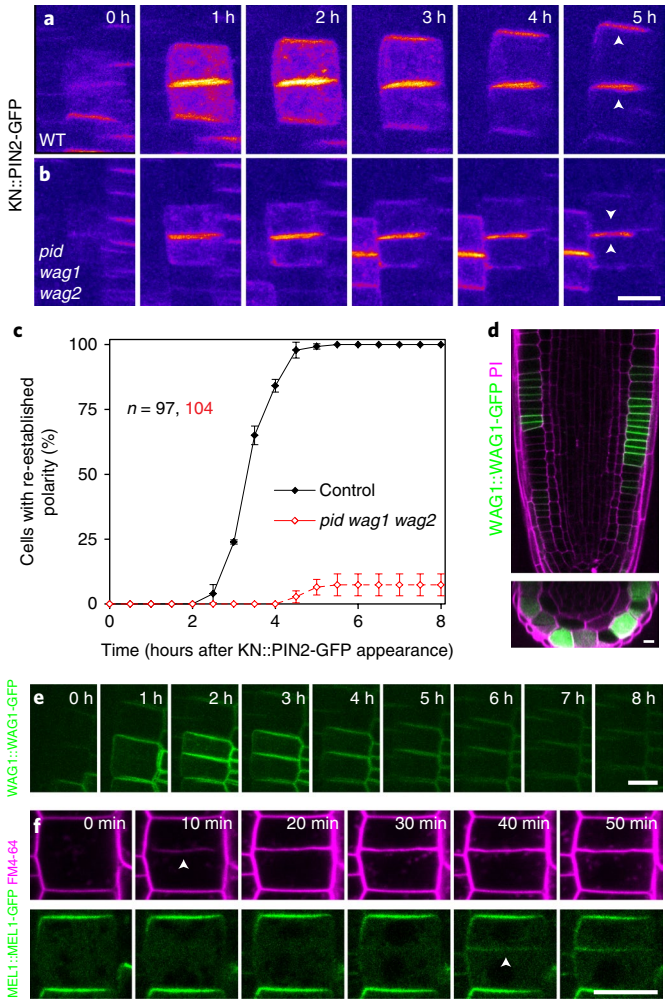

Fig. 4 | PIN apical polarity re-establishment is mediated by the AGCVIII kinase WAG1. a,**b**, *KN::PIN2-GFP* cells failed to re-establish apical polarity in the *pid wag1 wag2* triple mutant background. Arrowheads indicate predominant localization of PIN2-GFP. **c**, Quantitative analysis of **a** and **b**. The control is the same as in Fig. 1f. The graph shows mean ± s.d. of three independent experiments, *n* indicates the total number of cell pairs. The number of roots/cell pairs analysed in each experiment was 4/30, 4/38 and 4/36. **d**,**e**, Expression analysis of *WAG1::WAG1-GFP*. The signal is strongly and specifically increased in dividing cells exclusively in the epidermis. *XY* (top) and *XZ* (bottom) sections through the same root (**d**) and a time lapse of a single dividing cell from a different root (**e**) are shown. *n* > 100 cells from 16 roots in four independent experiments. **f**, Subcellular localization of MEL1::MEL1-GFP in dividing cells stained with FM4-64. MEL1-GFP never appears at the cell plate and can be detected only at the newly formed apical plasma membrane at >30 min after cell division. Arrowheads indicate the first appearance of the cell plate and of MEL1-GFP at the new plasma membrane, respectively. *n* = 80 cells from 18 roots in three independent experiments. Scale bars, 10 µm.

or additional polarity regulators[28–30]. Notably, analysis of the expression dynamics revealed that the abundance of WAG1 was strongly upregulated specifically in dividing epidermal cells (Fig. 4d,e and Supplementary Video 5).

Together, these results show that the cell cycle-regulated WAG1 and its homologues PID and WAG2 play a key role in PIN2 post-cytokinetic polarity re-establishment, explaining the previously reported pronounced PIN2 polarity defect in the *pid wag1 wag2* roots[6].

PID/WAG kinases have been shown to interact genetically with *MEL* genes encoding NPH3-like proteins of unknown function[31]. Notably, the membrane-associated MEL proteins co-localize with PINs and polarity of PINs is reduced in higher order *mel* mutants[31]. This prompted us to analyse the dynamic localization of the *MEL1-GFP* reporter in dividing epidermal cells. We detected MEL1-GFP localization at the apical plasma membrane of the mother cell and in the cytoplasm, but not at the cell plate. MEL1-GFP first appeared at the newly formed apical domain not before 30 minutes after cell division (Fig. 4f), presumably after it had lost cell plate and acquired plasma membrane identity. This localization pattern is a manifestation of the cell-intrinsic polarity cue inherited from the mother cell during cytokinesis and defining the apical domain of the daughter cell.

Maintenance of individual cell polarities over repeated rounds of cell division is crucial for tissue polarity and proper development in multicellular organisms. We show here that redefinition of the root epidermal cell apical–basal polarity after cell division is achieved in a cell-intrinsic manner. Subsequent PIN2 polarity re-establishment requires de novo protein secretion, CME and the activity of cell cycle-regulated WAG1 and related AGCVIII kinases. On the other hand, our detailed analysis does not support a major contribution of basal-to-apical transcytosis to re-establishment of PIN2 polarity. Based on our findings, we propose the following model: (1) During cytokinesis and in the first hour thereafter, PIN2 targeting is redirected to the cell plate along with most endomembrane traffic;[12] (2) PIN2 molecules localized ectopically to the basal side of the upper cell must be endocytosed, but are gradually turned over rather than being transcytosed to the apical side; and (3) During cytokinesis, WAG1 kinase is transcriptionally upregulated and together with its homologues is required for re-establishment of PIN2 localization to the apical plasma membrane, which is marked by the presence of MEL proteins. It remains a challenge for future investigations to elucidate the precise molecular machinery responsible for differential endocytosis rates between the apical and other plasma membrane domains, and to uncover the nature of the cell-intrinsic polarity cue responsible for proper redefinition of apical–basal polarity of newly divided cells.

Methods

Plant material and growth conditions. Seeds were surface sterilized by chlorine vapour, sown on ½ MurashigeSkoog medium supplemented with 1% sucrose and 1% agar and grown in vitro under long day conditions. The transgenic lines *PIN2::PIN2-Dendra*[32], *PIN2::nls-GFP*[32], *PIN2::PIN2-GFP*[8], *PIN2::PIN2-mCherry*[32] and *WAG1::WAG1-GFP*[6] were described previously. The lines *PIN2::Dendra-PIP1;4*, *KN::PIN2-GFP*, *KN::PIN2-Dendra*, *KN::PIN2^{S3A}-GFP* and *MEL1::MEL1-GFP* were generated by transformation of the respective constructs into *Col-0* by the floral dip method[33]. *KN::PIN2-GFP* was introduced into the *eir1–1*[34], *XVE»AXL2*[24], *pid wag1 wag2*[6], *big3*[12] *and XVE»DN-DRP1a-mRFP*[6] backgrounds by genetic crossing. In the case of *KN::PIN2-GFP* x *pid wag1 wag2*, *pid*$^{\pm}$ *wag1 wag2* plants were used for the cross. *pid*$^{\pm}$ plants were identified by PCR-based genotyping in F1 and F2 generations, and seedlings were selected based on the no cotyledon phenotype from an F3 *KN::PIN2-GFP*$^{+}$ x *pid*$^{\pm}$*wag1*$^{-/-}$*wag2*$^{-/-}$ line for the experiments. Due to high levels of *XVE»DN-DRP1a-mRFP* silencing, the construct was retransformed in our laboratory, T1 plants were used for the cross and the resulting F1/T2 plants were used for the experiments.

Molecular cloning. All cloning was performed using the Gateway Technology (Invitrogen). To generate *KN::PIN2-GFP*, a promoter fragment 1 kilobase (kb) upstream of the KNOLLE (*At1g08560*) start codon was cloned into pDONR P4-P1r, the *PIN2-GFP* coding sequence was cloned into pDONR 221 and both entry clones were recombined into the binary vector pB7m24GW,3. *KN::PIN2-Dendra* was generated analogically. To introduce S3A mutations into the *PIN2-GFP* sequence, an N-terminal *PIN2* fragment containing the three mutations was amplified from the *PIN:: PIN2^{S3A}-Venus* line genomic DNA[6], fused to a C-terminal fragment containing the *GFP* tag by overlap PCR, and cloned into pDONR 221, which was used to generate *KN::PIN2^{S3A}-GFP*. For *MEL1::MEL1-GFP*, a 2.9 kb fragment upstream of the *MEL1* (*At4g37590*) start codon was cloned into pDONR P4-P1r, the *MEL1* coding sequence without a stop codon into pDONR 221 and the *EGFP* coding sequence into pDONR P2r-P3. All three entry clones were then

recombined into pH7m34GW,0. *PIN2::Dendra-PIP1;4* was generated analogically by recombining the 1,397 base pair (bp) *PIN2* promoter in pDONR P4-P1r, the *Dendra* coding sequence without a stop codon in pDONR 221 and the *PIP1;4* coding sequence in pDONR P2r-P3 into pB7m34GW,0. Sequences of all primers used can be found in Supplementary Table 1.

Imaging and image analysis. Four-day-old seedlings were mounted on a slice of growth medium, containing the respective chemicals in case of pharmacological experiments, placed into a chambered coverslip (Lab-Tek) and imaged with Zeiss LSM700, LSM800 or LSM880 inverted confocal microscopes; long time lapse imaging was performed using a vertically oriented LSM700 microscope as described previously[35]. To apply chemical treatments, the respective amount of compound stock solution was predissolved in 100 µl H_2O, pipetted on to a slice of growth medium and incubated for 1–2 h at room temperature to diffuse. The seedlings were then transferred into a chambered coverslip (Lab-Tek), covered with the treatment-including medium and imaged, in the case of inhibitors together with a mock control containing only the solvent. The drugs (manufacturer; stock concentration and solvent; final concentration) were as follows: naphthylphthalamic acid (Duchefa; 10 mM dimethylsulfoxide (DMSO); 10 µM), indole-3-acetic acid (Sigma-Aldrich, 10 mM ethanol; 100 nM), β-estradiol (Sigma-Aldrich; 10 mM DMSO; 10 µM), brefeldin A (Sigma-Aldrich; 50 mM DMSO; 25 µM), cycloheximide (Sigma-Aldrich; 50 mM DMSO; 25 µM), propidium iodide (Sigma-Aldrich; 1 mg ml^{-1} H_2O; 50 µg ml^{-1}), FM4–64 (Invitrogen; 2 mM H_2O; 2 µM). In tissue context disruption experiments, roots mounted on growth medium were cut manually with a razor blade under a stereomicroscope. Individual cells were ablated with a 355 nm pulsed laser at a Zeiss Observer inverted microscope equipped with an Andor iXon 897 Spinning Disk system, propidium iodide was used to mark the ablated cells. Dendra photoconversion was performed as described previously[36]. Images were handled and analysed with FIJI[37] and Adobe Photoshop. All *KN::PIN2-GFP* time lapse data are presented as maximum intensity projections of a *Z* stack.

Phenotypic analysis. Plates with four-day-old light-grown seedlings were scanned on an Epson Perfection V700 flatbed scanner and root vertical growth index was measured as described previously[38].

Reproducibility and statistics. The number of independent repetitions of experiments, as well as exact sample sizes, is described in the figure legends. Tukey box plots were generated with BoxPlotR (http://shiny.chemgrid.org/boxplotr/). Statistical significance was tested as described in the figure legends. For the purpose of statistical analysis of KNOLLE::PIN2-GFP experiments, any cell pair that failed to repolarize during the time course of the experiment was considered to have repolarized after 10 h.

Reporting Summary. Further information on research design is available in the Nature Research Reporting Summary linked to this article.

Data availability

The data that support the findings of this study are available from the corresponding author upon request.

Received: 6 June 2018; Accepted: 1 November 2018;
Published online: 3 December 2018

References

1. Smertenko, A. et al. Plant cytokinesis: terminology for structures and processes. *Trends Cell Biol.* **27**, 885–894 (2017).
2. Geldner, N. et al. Auxin transport inhibitors block PIN1 cycling and vesicle trafficking. *Nature* **413**, 425–428 (2001).
3. Mravec, J. et al. Cell plate restricted association of DRP1A and PIN proteins is required for cell polarity establishment in *Arabidopsis*. *Curr. Biol.* **21**, 1055–1060 (2011).
4. Men, S. et al. Sterol-dependent endocytosis mediates post-cytokinetic acquisition of PIN2 auxin efflux carrier polarity. *Nat. Cell Biol.* **10**, 237–244 (2008).
5. Yoshinari, A. et al. DRP1-dependent endocytosis is essential for polar localization and boron-induced degradation of the borate transporter BOR1 in *Arabidopsis thaliana*. *Plant Cell Physiol.* **57**, 1985–2000 (2016).
6. Dhonukshe, P. et al. Plasma membrane-bound AGC3 kinases phosphorylate PIN auxin carriers at TPRXS(N/S) motifs to direct apical PIN recycling. *Development* **137**, 3245–3255 (2010).
7. Kania, U. et al. Polar delivery in plants; commonalities and differences to animal epithelial cells. *Open Biol.* **4**, 140017 (2014).
8. Abas, L. et al. Intracellular trafficking and proteolysis of the *Arabidopsis* auxin-efflux facilitator PIN2 are involved in root gravitropism. *Nat. Cell Biol.* **8**, 249–256 (2006).
9. Baster, P. et al. SCF(TIR1/AFB)-auxin signalling regulates PIN vacuolar trafficking and auxin fluxes during root gravitropism. *EMBO J.* **32**, 260–274 (2013).
10. Dhonukshe, P. et al. Endocytosis of cell surface material mediates cell plate formation during plant cytokinesis. *Dev. Cell* **10**, 137–150 (2006).
11. Gurskaya, N. G. et al. Engineering of a monomeric green-to-red photoactivatable fluorescent protein induced by blue light. *Nat. Biotechnol.* **24**, 461–465 (2006).
12. Richter, S. et al. Delivery of endocytosed proteins to the cell-division plane requires change of pathway from recycling to secretion. *eLife* **3**, e02131 (2014).
13. Lauber, M. H. et al. The *Arabidopsis* KNOLLE protein is a cytokinesis-specific syntaxin. *J. Cell Biol.* **139**, 1485–1493 (1997).
14. Sparks, E. et al. Spatiotemporal signalling in plant development. *Nat. Rev. Genet.* **14**, 631–644 (2013).
15. Mazur, E. et al. Vascular cambium regeneration and vessel formation in wounded inflorescence stems of *Arabidopsis*. *Sci. Rep.* **6**, 33754 (2016).
16. Prát, T. et al. WRKY23 is a component of the transcriptional network mediating auxin feedback on PIN polarity. *PLoS Genet.* **14**, e1007177 (2018).
17. Simon, S. et al. Defining the selectivity of processes along the auxin response chain: a study using auxin analogues. *New Phytol.* **200**, 1034–1048 (2013).
18. Sena, G. et al. Organ regeneration does not require a functional stem cell niche in plants. *Nature* **457**, 1150–1153 (2009).
19. Kleine-Vehn, J. et al. Cellular and molecular requirements for polar PIN targeting and transcytosis in plants. *Mol. Plant* **1**, 1056–1066 (2008).
20. Kleine-Vehn, J. et al. Recycling, clustering, and endocytosis jointly maintain PIN auxin carrier polarity at the plasma membrane. *Mol. Syst. Biol.* **7**, 540 (2011).
21. Feraru, E. et al. PIN polarity maintenance by the cell wall in *Arabidopsis*. *Curr. Biol.* **21**, 338–343 (2011).
22. Martinière, A. et al. Cell wall constrains lateral diffusion of plant plasma-membrane proteins. *Proc. Natl Acad. Sci. USA* **109**, 12805–12810 (2012).
23. Kitakura, S. et al. Clathrin mediates endocytosis and polar distribution of PIN auxin transporters in *Arabidopsis*. *Plant Cell* **23**, 1920–1931 (2011).
24. Adamowski, M. et al. A functional study of AUXILIN-LIKE1 and 2, two putative clathrin uncoating factors in *Arabidopsis*. *Plant Cell* **30**, 700–716 (2018).
25. Friml, J. et al. A PINOID-dependent binary switch in apical-basal PIN polar targeting directs auxin efflux. *Science* **306**, 862–865 (2004).
26. Michniewicz, M. et al. Antagonistic regulation of PIN phosphorylation by PP2A and PINOID directs auxin flux. *Cell* **130**, 1044–1056 (2007).
27. Kleine-Vehn, J. et al. PIN auxin efflux carrier polarity is regulated by PINOID kinase-mediated recruitment into GNOM-independent trafficking in *Arabidopsis*. *Plant Cell* **21**, 3839–3849 (2009).
28. Zhang, J. et al. PIN phosphorylation is sufficient to mediate PIN polarity and direct auxin transport. *Proc. Natl Acad. Sci. USA* **107**, 918–922 (2010).
29. Huang, F. et al. Phosphorylation of conserved PIN motifs directs *Arabidopsis* PIN1 polarity and auxin transport. *Plant Cell* **22**, 1129–1142 (2010).
30. Weller, B. et al. Dynamic PIN-FORMED auxin efflux carrier phosphorylation at the plasma membrane controls auxin efflux-dependent growth. *Proc. Natl Acad. Sci. USA* **114**, E887–E896 (2017).
31. Furutani, M. et al. Polar-localized NPH3-like proteins regulate polarity and endocytosis of PIN-FORMED auxin efflux carriers. *Development* **138**, 2069–2078 (2011).
32. Salanenka, Y. et al. Gibberellin DELLA signaling targets the retromer complex to redirect protein trafficking to the plasma membrane. *Proc. Natl Acad. Sci. USA* **115**, 3716–3721 (2018).
33. Clough, S. J. & Bent, A. F. Floral dip: a simplified method for Agrobacterium-mediated transformation of *Arabidopsis thaliana*. *Plant J.* **16**, 735–743 (1998).
34. Luschnig, C. et al. EIR1, a root-specific protein involved in auxin transport, is required for gravitropism in *Arabidopsis thaliana*. *Genes Dev.* **12**, 2175–2187 (1998).
35. von Wangenheim, D. et al. Live tracking of moving samples in confocal microscopy for vertically grown roots. *eLife* **6**, e26792 (2017).
36. Jásik, J. et al. PIN2 turnover in *Arabidopsis* root epidermal cells explored by the photoconvertible protein Dendra2. *PLoS ONE* **8**, e61403 (2013).
37. Schindelin, J. et al. Fiji: an open-source platform for biological-image analysis. *Nat. Methods* **9**, 676–682 (2012).
38. Grabov, A. et al. Morphometric analysis of root shape. *New Phytol.* **165**, 641–651 (2005).

Acknowledgements

We thank N. Geldner, C. Luschnig, G. Jürgens, R. Offringa and Y. Takano for sharing published material. We would also like to acknowledge M. Adamowski, U. Kania and

C. Cuesta for providing entry clones, and the Biomaging Facility at IST Austria for providing excellent imaging service and assistance. The research leading to these results has received funding from the European Research Council under the European Union's Seventh Framework Programme/ERC grant agreement no. 742985. Additionally, funding was received from the Ministry of Education of the Czech Republic/MŠMT project NPUI - LO1417.

Author contributions

M.G. designed experiments, performed experiments, analysed data and wrote the manuscript. M.F. designed experiments, analysed data and edited the manuscript. J.F. initiated the project, acquired funding, designed experiments and wrote the manuscript.

Competing interests

The authors declare no competing interests.

Additional information

Supplementary information is available for this paper at https://doi.org/10.1038/s41477-018-0318-3.

Reprints and permissions information is available at www.nature.com/reprints.

Correspondence and requests for materials should be addressed to J.F.

nature research

Corresponding author(s): Jiří Friml

Reporting Summary

Nature Research wishes to improve the reproducibility of the work that we publish. This form provides structure for consistency and transparency in reporting. For further information on Nature Research policies, see Authors & Referees and the Editorial Policy Checklist.

Statistical parameters

When statistical analyses are reported, confirm that the following items are present in the relevant location (e.g. figure legend, table legend, main text, or Methods section).

n/a	Confirmed	
☐	☒	The exact sample size (*n*) for each experimental group/condition, given as a discrete number and unit of measurement
☐	☒	An indication of whether measurements were taken from distinct samples or whether the same sample was measured repeatedly
☐	☒	The statistical test(s) used AND whether they are one- or two-sided *Only common tests should be described solely by name; describe more complex techniques in the Methods section.*
☒	☐	A description of all covariates tested
☐	☒	A description of any assumptions or corrections, such as tests of normality and adjustment for multiple comparisons
☐	☒	A full description of the statistics including central tendency (e.g. means) or other basic estimates (e.g. regression coefficient) AND variation (e.g. standard deviation) or associated estimates of uncertainty (e.g. confidence intervals)
☒	☐	For null hypothesis testing, the test statistic (e.g. *F*, *t*, *r*) with confidence intervals, effect sizes, degrees of freedom and *P* value noted *Give P values as exact values whenever suitable.*
☒	☐	For Bayesian analysis, information on the choice of priors and Markov chain Monte Carlo settings
☒	☐	For hierarchical and complex designs, identification of the appropriate level for tests and full reporting of outcomes
☒	☐	Estimates of effect sizes (e.g. Cohen's *d*, Pearson's *r*), indicating how they were calculated
☐	☒	Clearly defined error bars *State explicitly what error bars represent (e.g. SD, SE, CI)*

Our web collection on statistics for biologists may be useful.

Software and code

Policy information about availability of computer code

Data collection	The TipTracker script that was used to collect data was described previously (von Wangenheim et al., 2017; https://doi.org/10.7554/eLife.26792.022)
Data analysis	Following software was used to analyze data: FIJI / ImageJ v 1.51w; Microsoft Excel 2010 and 2016; BoxPlotR (http://shiny.chemgrid.org/boxplotr/); RStudio 1.1.383. Figures were assembled using Adobe Photoshop CS5, Adobe Illustrator CS5 and CC, and LibreOffice Draw 6.1.0.3.

For manuscripts utilizing custom algorithms or software that are central to the research but not yet described in published literature, software must be made available to editors/reviewers upon request. We strongly encourage code deposition in a community repository (e.g. GitHub). See the Nature Research guidelines for submitting code & software for further information.

Data

Policy information about availability of data

All manuscripts must include a data availability statement. This statement should provide the following information, where applicable:

- Accession codes, unique identifiers, or web links for publicly available datasets
- A list of figures that have associated raw data
- A description of any restrictions on data availability

The datasets generated during and/or analysed during the current study are available from the corresponding author on reasonable request.

Field-specific reporting

Please select the best fit for your research. If you are not sure, read the appropriate sections before making your selection.

☒ Life sciences ☐ Behavioural & social sciences ☐ Ecological, evolutionary & environmental sciences

For a reference copy of the document with all sections, see nature.com/authors/policies/ReportingSummary-flat.pdf

Life sciences study design

All studies must disclose on these points even when the disclosure is negative.

Sample size	No statistical methods were used to predetermine sample size; sample size was determined empirically throughout experiments as an optimal trade-off between sample size, image quality and feasibility in each particular epxeriment. The sample sizes were considered sufficient sice all observed trends were consistent between samples within an experiment as well as between independent experimental replicates.
Data exclusions	No data was excluded from the analysis
Replication	Each experiment was repeated 2-4 times and all attempts at replication were successful
Randomization	Selecting seedlings for mock/experimental treatments and/or imaging from a plate containing at least one order of magnitude more individuals than needed for the experiment was inherently random; no other randomization method was used.
Blinding	Blinding was not possible due to the effects of each mutation/treatment on the growth and/or morphology of the plants that were obvious at first sight.

Reporting for specific materials, systems and methods

Materials & experimental systems

n/a	Involved in the study
☐	☒ Unique biological materials
☒	☐ Antibodies
☒	☐ Eukaryotic cell lines
☒	☐ Palaeontology
☒	☐ Animals and other organisms
☒	☐ Human research participants

Methods

n/a	Involved in the study
☒	☐ ChIP-seq
☒	☐ Flow cytometry
☒	☐ MRI-based neuroimaging

Unique biological materials

Policy information about availability of materials

Obtaining unique materials	All unique biological materials (Arabidopsis transgenic lines and DNA constructs) are available from the corresponding author with the exception of the KN::PIN2-GFP x XVE>>DRP1a-mRFP line, since F1 seeds were used in this case and their amount is thus very limited. Upon request, KN::PIN2-GFP seeds and XVE>>DRP1a-mRFP expression clone (also available from Yunpei Takano, corresponding author of Yoshinari et al., 2016, where the construct was described) can be provided instead so that the line can be re-created as described in Materials and Methods.